Available online at www.sciencedirect.com
SCIENCE DIRECT®
Journal of Solid State Chemistry 177 (2004) 901–908
JOURNAL OF SOLID STATE CHEMISTRY
http://elsevier.com/locate/jssc

# Photoluminescence of $Ce^{3+}$, $Pr^{3+}$ and $Tb^{3+}$ activated $Sr_3Ln(PO_4)_3$ under VUV-UV excitation

Hongbin Liang,[a] Ye Tao,[b] Jianhua Xu,[b] Hong He,[c] Hao Wu,[a] Wenxuan Chen,[a] Shubin Wang,[c] and Qiang Su[a,c,*]

[a] *State Key Laboratory of Optoelectronic Materials and Technologies, School of Chemistry and Chemical Engineering, Sun Yat-Sen University, Guangzhou, Guangdong 510275, People's Republic of China*

[b] *Laboratory of Beijing Synchrotron Radiation, Institute of High Energy Physics, Chinese Academy of Sciences, Beijing 100039, People's Republic of China*

[c] *Key Laboratory of Rare Earth Chemistry and Physics, Changchun Institute of Applied Chemistry, Chinese Academy of Sciences, Changchun, Jilin 130022, People's Republic of China*

Received 18 June 2003; received in revised form 3 September 2003; accepted 23 September 2003

**Abstract**

The spectroscopic properties in VUV-Vis range for the eulytite structural phosphors $Sr_3Gd(PO_4)_3$:$Ln^{3+}$ ($Ln^{3+}=Ce^{3+}$, $Pr^{3+}$, $Tb^{3+}$), $Sr_3Ce(PO_4)_3$, $Sr_3Gd(PO_4)_3$ and $Sr_3Tb(PO_4)_3$ were investigated. The bands near 170 nm in VUV excitation spectra are assumed to connect with the host lattices related absorption. The *f–d* transitions of $Ce^{3+}$, $Pr^{3+}$ and $Tb^{3+}$ in the host lattices are assigned and corroborated. A convenient experiment formulation on the relationship between the lowest *f–d* transition energies and *n* value for trivalent $4f^n$-series rare earth ions in these host lattices is applied.


*Keywords:* Luminescence; Eulytite; Lanthanide; Rare earth; Phosphates

## 1. Introduction

Ternary orthophosphates $Sr_3Ln(PO_4)_3$ belong to the large family of eulytite (also called eulytine or agricolite) compounds. The structural type of eulytite was first recognized in the mineral $Bi_4(SiO_4)_3$ (BSO). It is cubic space group, with Bi in the 16*c*, Si in the 12*a* and O in the 48*e* equipoints of space group $I\bar{4}3d$. There are four formula units in the unit cell [1]. Potential and effective technological applications have significantly revived interest in new materials crystallizing with eulytite structure. A large number of compounds isostructural with this mineral, for example, $Bi_4(GeO_4)_3$ (BGO), $Pb_3Bi(XO_4)_3$ ($X=P$, As, V), $M_3RE(PO_4)_3$ ($M=Ca$, Sr, Ba; $RE=$rare earth) and $Ba_3Bi(PO_4)_3$ have been reported over the past years [2–7].

As far as spectroscopic properties are concerned, attention has been brought to eulytite structural phosphates doped with rare earth ions. Hoogendorp et al. reported the luminescence of $M_3La(PO_4)_3$:$Ce^{3+}$ ($M=$Sr, Ba) under UV excitation [8]. The possible application of $Ba_3Y(PO_5)_3$:$Nd^{3+}$ as powder laser materials was discussed by Znamierowska et al. [9]. However, to our knowledge, the photoluminescence of rare earth-doped eulytite structural phosphates under VUV (vacuum ultraviolet, $E>50,000\,cm^{-1}$) excitation has not been reported so far.

Some investigations on the luminescent properties under VUV excitation of rare earth activated fluorides and oxides have been performed. These investigations are very important from the standpoint of the development of (V)UV tunable laser materials, scintillators, and intense luminescent materials which are applicable to the phosphors used in mercury-free lamp or plasma display panels (PDP) [10–12]. The design of phosphors optimized for PDP or the mercury-free lamp involves a new set of considerations that is not included in the development of traditional lamp phosphors. The plasma

*Corresponding author. Key Laboratory of Rare Earth Chemistry and Physics, Changchun Institute of Applied Chemistry, Chinese Academy of Sciences, Changchun, Jilin 130022, People's Republic of China. Fax: +86-431-5698041.

*E-mail addresses:* hbliang888@yahoo.com, cedc25@zsu.edu.cn (H. Liang), suqiang@ciac.jl.cn (Q. Su).

0022-4596/$ - see front matter © 2003 Elsevier Inc. All rights reserved.
doi:10.1016/j.jssc.2003.09.037

of xenon containing noble gas mixture provides the excitation in a PDP or mercury-free lamp. The main emission of this plasma consists of 147 and 172 nm bands. The requirement that the phosphor host lattice or activators must absorb efficiently around these wavelengths is setting up new restrictions on the materials to be investigated. In order to seek these materials, the spectroscopic properties of rare earth in VUV range must be well understood first. It is known that Dieke diagram was extended to about 65,000 $cm^{-1}$ by Meijerink's group recently [13,14]. However, the *f–d* transitions of the rare earth ions, which are dependent intensively on the host lattices, as well as the host lattice absorption are necessary for further investigations [15–18].

In this work we present investigations on the VUV-Vis range spectroscopic properties of $Sr_3Gd(PO_4)_3$, $Sr_3Ln(PO_4)_3$ ($Ln$ = Ce, Tb), and $Ce^{3+}$, $Pr^{3+}$, $Tb^{3+}$ activated $Sr_3Gd(PO_4)_3$ phosphors.

## 2. Experimental section

The samples were prepared using high temperature solid-state reaction technique. The reactants include analytical grade pure $SrCO_3$, $NH_4H_2PO_4$ and 99.9% pure rare earth oxides $CeO_2$, $Pr_6O_{11}$, $Gd_2O_3$ and $Tb_4O_7$. According to the nominal compositions of compounds $Sr_3Gd_{1-x}Ln_x(PO_4)_3$ ($Ln^{3+}$ = $Ce^{3+}$, $Pr^{3+}$, $Tb^{3+}$; $x$ = 0.00−0.06), $Sr_3Ce(PO_4)_3$ and $Sr_3Tb(PO_4)_3$, appropriate amount of starting materials were thoroughly mixed and ground, and subsequently the mixture was pre-fired at 600°C for 2 h. After milling for a second time, the sample were calcined at 1250°C in air [for sample $Sr_3Gd(PO_4)_3$] or CO reducing atmosphere, [for the samples $Sr_3Ce(PO_4)_3$, $Sr_3Tb(PO_4)_3$, and $Sr_3Gd(PO_4)_3$:$Ln^{3+}$ ($Ln^{3+}$ = $Ce^{3+}$, $Pr^{3+}$, $Tb^{3+}$)], respectively. After these steps the temperature was slowly cooled down to the room temperature.

The structure of prepared samples was checked by X-ray powder diffraction using Cu$K\alpha$ radiation and the XRD data indicated that the samples were single cubic phases and in good agreement with those in JCPDS cards 29-1298 [$Sr_3Ce(PO_4)_3$], 29-1301 [$Sr_3Gd(PO_4)_3$] and 33-1353 [$Sr_3Tb(PO_4)_3$], respectively.

UV excitation spectra and UV excited luminescent spectra were recorded on a SPEX 2T2 spectrofluorometer equipped with 0.22 m SPEX 1680 double monochromators at room temperature, and a 450 W xenon lamp as excitation source.

The VUV excitation and VUV excited emission spectra were measured at the VUV spectroscopic experimental station on beamline 3B1B, Beijing Synchrotron Radiation Facilities (BSRF), under high-energy physics mode (1.8 GeV, 30–40 mA) at 293 K. A Seya type VUV monochromator (1200 g/mm) was used to provide the excitation VUV light, while an ARC SP-308 monochromator was used for the emission spectra. The optical signal was detected by a Hamamatsu H6240 photomultiplier. The relative VUV excitation intensities of the samples were corrected by dividing the measured excitation intensities of the samples with that of sodium salicylate under the same measurement conditions. The vacuum level in the sample chamber was around $2 \times 10^{-5}$ mbar.

## 3. Results and discussion

### 3.1. The spectroscopic properties of $Sr_3Gd(PO_4)_3$

Fig. 1 shows the VUV-UV excitation spectra and VUV-UV excited emission spectra of the sample $Sr_3Gd(PO_4)_3$. The main purpose we determine the spectra of $Sr_3Gd(PO_4)_3$ is to corroborate the energy of the host absorption band. The dominant band with a maximum at 170 nm in VUV excitation curve (solid line a) is assignable to a host excitation related band, namely, the transition energy between conduct band and valence band of $PO_4^{3-}$ group or the absorption due

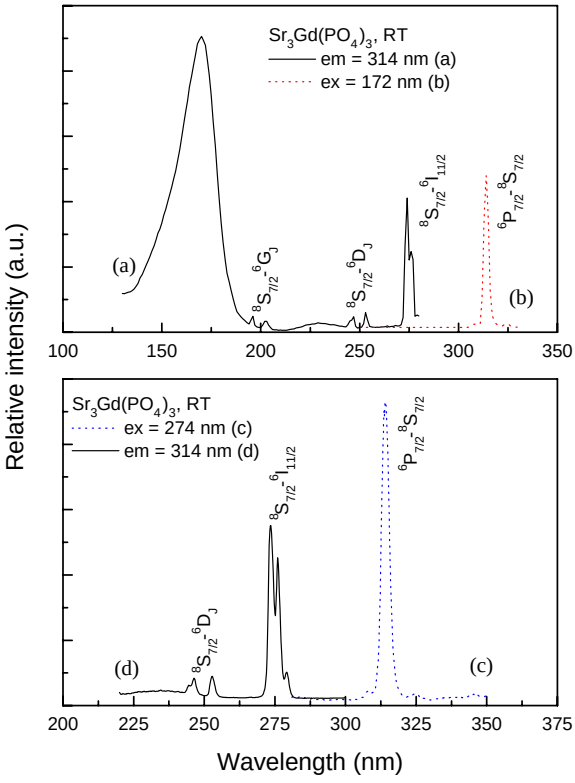


Fig. 1. The VUV excitation spectrum ((a) under emission at 314 nm), VUV excited emission spectrum ((b) excitation under 172 nm), UV excitation spectrum ((d) under emission at 314 nm) and UV excited emission spectrum ((c) excitation under 274 nm) of phosphor $Sr_3Gd(PO_4)_3$ at 293 K.

Table 1
The host related absorption band of phosphors $Sr_3Gd_{1-x}Ln_x(PO_4)_3$ ($Ln^{3+}=Ce^{3+}$, $Pr^{3+}$, $Tb^{3+}$, $x=0.00$, 0.06), $Sr_3Ce(PO_4)_3$ and $Sr_3Tb(PO_4)_3$

| Phosphor | Figure | Band position (nm) |
|---|---|---|
| $Sr_3Gd(PO_4)_3$ | 1 | 172 |
| $Sr_3Ce(PO_4)_3$ | 2 | 168 |
| $Sr_3Gd(PO_4)_3:Ce^{3+}$ | 3 | 170 |
| $Sr_3Gd(PO_4)_3:Pr^{3+}$ | 4 | 172 |
| $Sr_3Tb(PO_4)_3$ | 5 | 175 |
| $Sr_3Gd(PO_4)_3:Tb^{3+}$ | 6 | 173 |

to near-excitonic and impurity in $Sr_3Gd(PO_4)_3$. Generally speaking, the band-to-band transition energy of a definite host lattice is an intrinsic property of this compound; therefore, it has no considerable change when the different activators were doped. In order to confirm the attribution of this band, the optical spectra of $Sr_3Gd_{1-x}(PO_4)_3:xLn^{3+}$ ($Ln^{3+}=Ce^{3+}$, $Pr^{3+}$, $Tb^{3+}$, $x=0.00-0.06$), $Sr_3Ce(PO_4)_3$ and $Sr_3Tb(PO_4)_3$ were performed and the observed host absorption bands are listed in Table 1, it can be found that the change of the doped ions have no considerable influence on this energy, all of the samples exhibit the bands near 170 nm, this wavelength is very close to the emission wavelength of Xe containing noble gases plasma. The host related absorption bands of rare earth orthophosphates [19,20] were calculated to be about 7.0–7.8 eV, which is near our results.

The *f–f* transitions of $Gd^{3+}$ can also be observed in VUV excitation spectrum, $^8S_{7/2}$–$^6G_J$ transitions are with the maxima around 200 nm, $^8S_{7/2}$–$^6D_J$ transition 250 nm and $^8S_{7/2}$–$^6I_{11/2}$ 274 nm. The latter two groups of transitions were also found in UV excitation curve, the VUV excitation curve is in good agreement with the UV excitation line in the range of 240–280 nm. Upon excitation the host absorption at 172 nm or direct excitation the $^8S_{7/2}$–$^6I_{11/2}$ transition of $Gd^{3+}$ at 274 nm, the emission spectra under VUV-UV excitation were obtained and the similar emission of $Gd^{3+}$ $^6P_{7/2}$–$^8S_{7/2}$ transition at 314 nm can be observed, as shown in curves b and c. It implies that the host lattice efficiently transfer energy to the activators.

### 3.2. The spectroscopic properties of $Sr_3Ce(PO_4)_3$ and $Sr_3Gd(PO_4)_3:Ce^{3+}$

In Fig. 2 the VUV excited emission spectrum (curve a), VUV excitation spectrum (curve b), UV excited emission spectrum (curve c) and UV excitation spectrum (curve d) for the sample $Sr_3Ce(PO_4)_3$ are plotted. The spectroscopic curves in 130–500 nm range for sample $Sr_3Gd(PO_4)_3$:Ce are presented in Fig. 3. The samples $Sr_3Ce(PO_4)_3$ and $Sr_3Gd(PO_4)_3:Ce^{3+}$ show strong emission band with the maximum around 370 nm

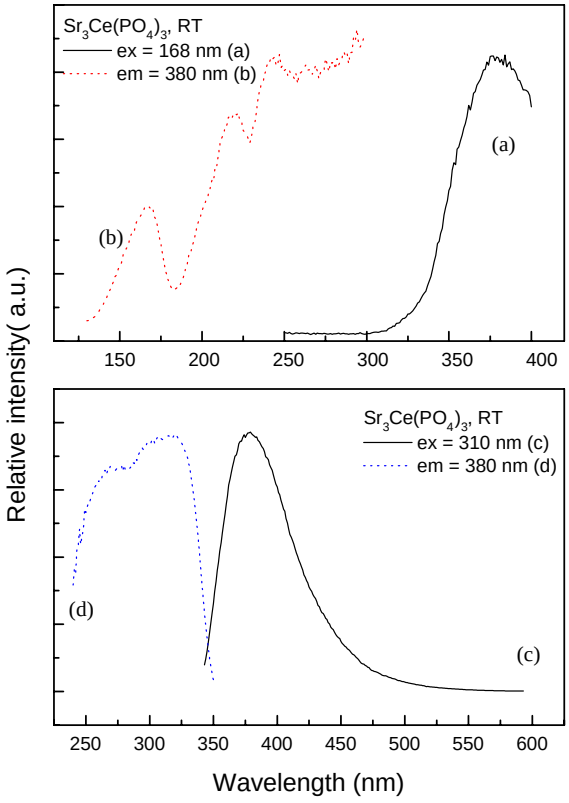


Fig. 2. The VUV excited emission spectrum ((a) excitation under 168 nm), VUV excitation spectrum ((b) under emission at 380 nm), UV excited emission spectrum ((c) excitation under 310 nm) and UV excitation spectrum ((d) under emission at 380 nm) of phosphor $Sr_3Ce(PO_4)_3$ at 293 K.

(27,027 $cm^{-1}$) under UV-VUV excitation, and the emission curves are rather broad with the full-width at half-maximum (FWHM) about $5\times10^3$ $cm^{-1}$, the characteristic splitting of the emission band of $Ce^{3+}$ due to the spin-orbit coupling is not observed. Upon 170 nm (the host absorption) VUV excitation, both the $Ce^{3+}$ and $Gd^{3+}$ ($^6P_{7/2}$–$^8S_{7/2}$, 314 nm) emission might be observed, which implied that the efficient energy transfer between host and $RE^{3+}$ occurred.

In 1994, Hoogendorp et al. reported the luminescent properties of $Ce^{3+}$ activated isostructural compounds, $M_3La(PO_4)_3:Ce^{3+}$ ($M$ = Sr, Ba), $Ba_{2.5}La_{1.5}(PO_4)_{2.5}(SiO_4)_{0.5}:Ce^{3+}$ and $Ba_4(PO_4)_2(SO_4):Ce^{3+}$ under UV excitation [8]. It was found that the astonishing broad emission and excitation bands are with the maxima at 375–380 and 315 nm for these phosphors, and it was suggested that $Ce^{3+}$ ions with variation surroundings which is comparable to that of a glass probably result in these remarkable broad emissions. Comparing our VUV-Vis spectroscopic results (emission at 370 nm and the lowest excitation at 310 nm) with Hoogendorp reported UV-Vis spectra, it could be found that the wavelengths of emission and lowest excitation band are close to one another for these isostructural phosphors. It

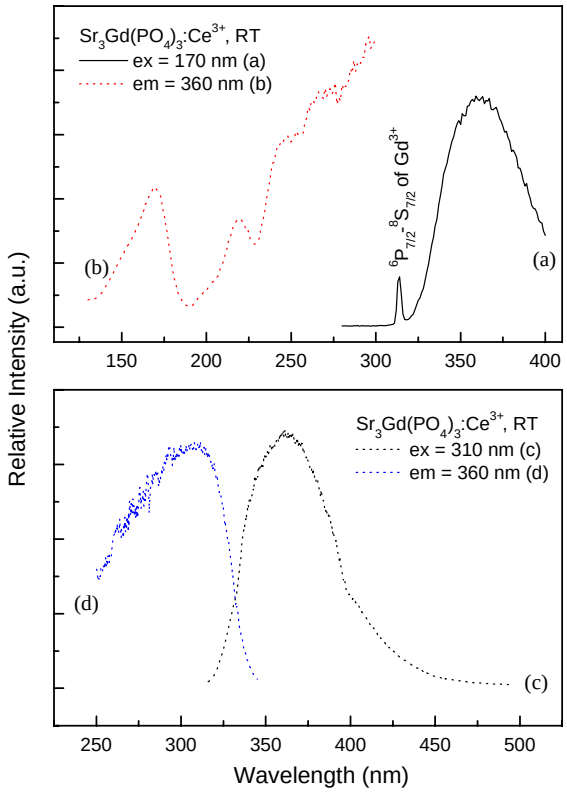


Fig. 3. The VUV excited emission spectrum ((a) excitation under 170 nm), VUV excitation spectrum ((b) under emission at 360 nm), UV excited emission spectrum ((c) excitation under 310 nm) and UV excitation spectrum ((d) under emission at 360 nm) of phosphor $Sr_3Gd_{0.94}Ce_{0.06}(PO_4)_3$ at 293 K.

seems that the dependence of the luminescence on the composition of these host lattices is small. In the prototypical eulytite compounds BGO and BSO, $Bi^{3+}$ ion occupies a distorted octahedron of oxygen ions. The site symmetry of $Bi^{3+}$ is $C_3$ symmetry [6,21]. For this structure, there is complete order due to the fact that the $Bi^{3+}$ ion requires an asymmetrical coordination with three short and three long Bi–O distances. The oxygen ions occupy one set of (48*e*) sites to satisfy this requirement. However, in $M_3Ln(PO_4)_3$ (*M*:alkaline earth metal ions) the cations do not have such specific bonding requirements and the oxygen ions are found equally disordered over three (48*e*) sites. The composition $M_3Ln(PO_4)_3$ was found to show not only a cation disorder ($M^{2+}/La^{3+}$ on $Bi^{3+}$ sites) but also an oxygen sublattice disorder [7,8]. In this way it can be imagined that each of the $Ce^{3+}$ ions seem to be able to choose its own coordination in $M_3Ln(PO_4)_3$, so that the emission bands are very broad and show small differences.

The smaller value of the energy difference between the emission and the excitation maximum can be used to represent the Stokes shift. Because the *f–d* bands of $Ce^{3+}$ in $Sr_3Ln(PO_4)_3$:$Ce^{3+}$ are remarkable broad, the Stokes shift is hard to be determined accurately. The lowest *f–d* transition excitation bands were observed around 310 nm (32,258 $cm^{-1}$) in Figs. 2(d) and 3(d); therefore, the Stokes shift is estimated to be near or slightly lower than $5\times10^3\,cm^{-1}$. The stokes shift of $Ce^{3+}$ in $YPO_4$:$Ce^{3+}$ was reported to be very small (550 $cm^{-1}$) [17]. In our previous work, this values are found to be 3000 $cm^{-1}$ for $Ce^{3+}$ in $Ba_3(PO_4)_2$:$Ce^{3+}$, 3800 $cm^{-1}$ in $Sr_3(PO_4)_2$:$Ce^{3+}$ and 2600 $cm^{-1}$ in $CaBPO_5$:$Ce^{3+}$ [22–24]. These results implied that the changes of ion-lattice coupling for these containing tetrahedral $PO_4^{3-}$ anions phosphates are as the following order: $Sr_3Ln(PO_4)_3$: $Ce^{3+}$ > $Sr_3(PO_4)_2$: $Ce^{3+}$ > $Ba_3(PO_4)_2$: $Ce^{3+}$ > $CaBPO_5$: $Ce^{3+}$ > $YPO_4$:$Ce^{3+}$.

The bands peaking at about 220 nm in VUV excitation curves are considered to connect with the highest *f–d* transitions of $Ce^{3+}$. This position is lower than that of $Ce^{3+}$ in $YPO_4$ (203 nm) [17]. The 5*d* crystal splitting components were not observed in the VUV-UV excitation spectra, this is in agreement with the above suggestions that each of $Ce^{3+}$ ions are probably able to dictate its own coordination in the hosts.

From the observed energy difference between the highest and lowest *f–d* transitions in VUV-UV excitation spectra, the crystal field splitting of 5*d* orbital for $Ce^{3+}$ in $Sr_3Ce(PO_4)_3$ and $Sr_3Gd(PO_4)_3$:$Ce^{3+}$ is calculated to be $13.0\times10^3\,cm^{-1}$, and the barycenter of the 4*f*5*d* levels calculated from the mean value of the highest and lowest excitation peaks is around $38.9\times10^3\,cm^{-1}$. The effect of crystal field on the 5*d* orbit will depress the lowest and the barycenter of the level energies in a specific host lattices compared to the free ions. It is known that the level energy of lowest 5*d* state for free $Ce^{3+}$ is 49,340 $cm^{-1}$, therefore, the lowest 5*d* level energy depresses around $17.0\times10^3\,cm^{-1}$. The centroid energy of free $Ce^{3+}$ ion was reported to be 51,230 $cm^{-1}$, hence the centroid shift for $Ce^{3+}$ in $Sr_3Ln(PO_4)_3$ is about $12.3\times10^3\,cm^{-1}$, this value is rather large for $Ce^{3+}$ in phosphates, for example, the value for $Ce^{3+}$ in $LnP_5O_{14}$ (*Ln* = La, Ce), $LaP_3O_9$, $REPO_4$ (*RE* = La, Y, Lu) and $K_3La(PO_4)_2$ is reported below $10.0\times10^3\,cm^{-1}$ [25]. The results exhibit that the binding of the ligand charge cloud to cations is smaller for $Sr_3Ln(PO_4)_3$:$Ce^{3+}$ due to the larger nephelauxetic effect. In principle, with the covalency and nephelauxetic effect increase, the attraction of cations to charge cloud decrease, which lead to the ion-lattice coupling increase, thus the barycenter of the 5*d* levels decline.

### 3.3. The spectroscopic properties of $Sr_3Gd(PO_4)_3$:$Pr^{3+}$

The emission spectra under 172 nm VUV and 274 nm UV excitation as well as VUV-UV excitation spectra under emission at 627 nm for the sample $Sr_3Gd_{0.94}Pr_{0.06}(PO_4)_3$ at room temperature are shown in curves a–d of Fig. 4. The band at 172 nm is the host lattice absorption, as described before. The bands in the range of 180–250 nm are related to the excitation of 4*f*5*d*

states, among these bands, the band with a maximum at 222 nm (45,045 $cm^{-1}$) is considered to be the lowest $4f^2 \rightarrow 4f^1 5d^1$ transition for $Pr^{3+}$ in the host lattice. Therefore, the lowest 5*d* level of $Pr^{3+}$ in $Sr_3Gd(PO_4)_3$ decreases about $16.5 \times 10^3$ $cm^{-1}$, comparing to the free ions (61,580 $cm^{-1}$). It is interested to noted that this red shift value of $Pr^{3+}$ in $Sr_3Gd(PO_4)_3$ is nearly equal to that of $Ce^{3+}$ in the same host lattice ($17 \times 10^3$) mentioned above. As demonstrated by Dorenbos in an extensive review on the position of 5*d* transitions of lanthanides, it is possible to use the position of the 5*d* levels of $Ce^{3+}$ to predict that of all other lanthanides [25–27]. This can be done because the influence of the crystal field and covalency of the host lattice on the red shift of 4*f*5*d* levels are approximately equal for all rare earth ions. This is true for $Ce^{3+}$ and $Pr^{3+}$ in $Sr_3Ln(PO_4)_3$. From the observed energy of the lowest 5*d* state and red shift for $Ce^{3+}$ in $Sr_3Ln(PO_4)_3$ (17,000 $cm^{-1}$), the lowest 5*d* level of $Pr^{3+}$ in this host lattice can be predicted to be 224 nm, this result is in line with the band we observed, which corroborates the attribution of this band.

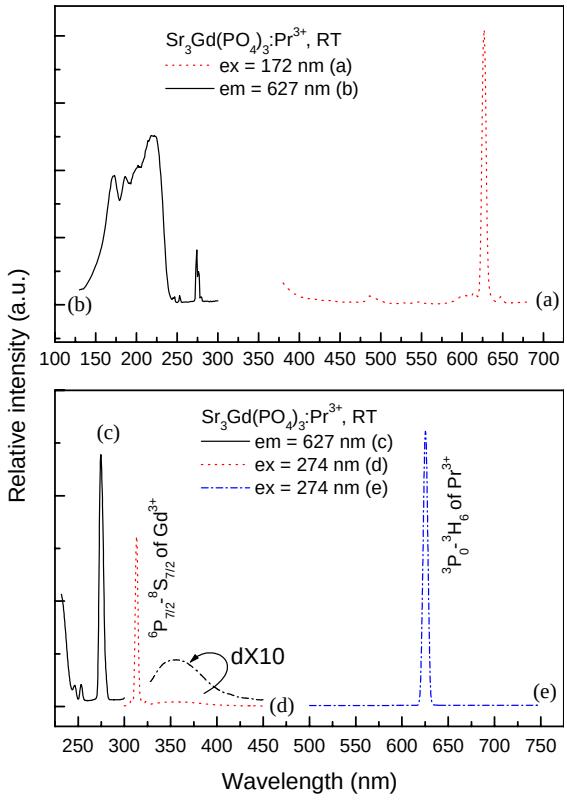


Fig. 4. The VUV excited emission spectrum ((a) excitation under 172 nm), VUV excitation spectrum ((b) under emission at 627 nm), UV excitation spectrum ((c) under emission at 627 nm), UV excited emission spectrum ((d and e) excitation under 274 nm) of phosphor $Sr_3Gd_{0.94}Pr_{0.06}(PO_4)_3$ at 293 K.

As the broad and parity-allowed *f*–*d* transitions overlap on the weak $^1S_0$–$^3H_4$ transition of $Pr^{3+}$, this *f*–*f* transition was not observed in VUV excitation spectrum. It is reported that the energy of $^1S_0$ level is about 46,450 $cm^{-1}$ (215 nm) for $Pr^{3+}$ in most oxides and fluorides host, obviously, it is higher than that of the lowest 5*d* level of $Pr^{3+}$ in $Sr_3Gd(PO_4)_3$, therefore, the photon cascade emission cannot occur in $Sr_3Gd(PO_4)_3$:$Pr^{3+}$ [28]. As shown in Fig. 4, upon excitation the host absorption band or $^8S_{7/2}$–$^6I_{11/2}$ transition of $Gd^{3+}$ at 274 nm, except the $^6P_{7/2} \rightarrow {}^8S_{7/2}$ emission transition of $Gd^{3+}$ peaking at 318 nm, a weak *d*–*f* transitions band at about 355 nm (most probably the traces of $Ce^{3+}$ impurities emission) and the *f*–*f* transitions around 488 nm ($^3P_0 \rightarrow {}^3H_4$), as well as the red emission at 628 nm ($^3P_0 \rightarrow {}^3H_6$) transition of $Pr^{3+}$ were observed. These emission spectra are similar with that of *B*GO:$Pr^{3+}$ [the prototypical eulytite compound of phosphates $Sr_3Ln(PO_4)_3$] under UV excitation [29]. The spectroscopic results imply that the energy transfer among the host lattice-$Gd^{3+}$-$Pr^{3+}$ occurred. The CIE (Commission Internationale de l'Eclairage, International Commission on Illumination) chromaticity coordinates of the National Television Standard Committee (NTSC) for red are $x = 0.67$, $y = 0.33$, the calculated chromaticity coordinates for the phosphor $Sr_3Gd(PO_4)_3$:$Pr^{3+}$ are listed in Table 2, showing there is a small difference with NTSC values.

### 3.4. The spectroscopic properties of $Sr_3Tb(PO_4)_3$ and $Sr_3Gd(PO_4)_3$:$Tb^{3+}$

The VUV excitation spectra, measurements at 293 K for the samples $Sr_3Tb(PO_4)_3$ and $Sr_3Gd_{0.94}Tb_{0.06}(PO_4)_3$ under $^5D_4$–$^7F_5$ emission of $Tb^{3+}$ are presented in Figs. 5 and 6, respectively. The host lattice absorption band near 170 nm can be observed in VUV excitation spectra and was listed in Table 1.

Table 2
The CIE coordination *x*, *y* values of $Sr_3Gd(PO_4)_3$:$Pr^{3+}$, $Sr_3Tb(PO_4)_3$ and $Sr_3Gd(PO_4)_3$:$Tb^{3+}$

| Excitation | $Sr_3Gd(PO_4)_3$:$Pr^{3+}$ | | $Sr_3Tb(PO_4)_3$ | | $Sr_3Gd(PO_4)_3$:$Tb^{3+}$ | |
|---|---|---|---|---|---|---|
| | *x* | *y* | *x* | *y* | *x* | *y* |
| | $\lambda_{ex} = 172$, 274 nm | | $\lambda_{ex} = 175$, 258 nm | | $\lambda_{ex} = 173$, 274 nm | |
| VUV | 0.57 | 0.29 | 0.28 | 0.59 | 0.24 | 0.45 |
| UV | 0.64 | 0.31 | 0.26 | 0.60 | 0.23 | 0.46 |

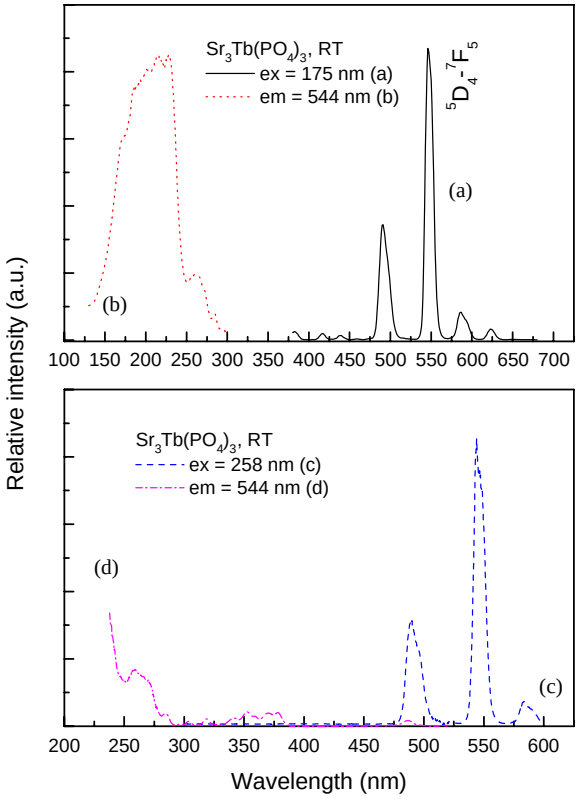


Fig. 5. The VUV excited emission spectrum ((a) excitation under 175 nm), VUV excitation spectrum ((b) under emission at 544 nm), UV excited emission spectrum ((c) excitation under 258 nm) and UV excitation spectrum ((d) under emission at 544 nm) of phosphor $Sr_3Tb(PO_4)_3$ at 293 K.

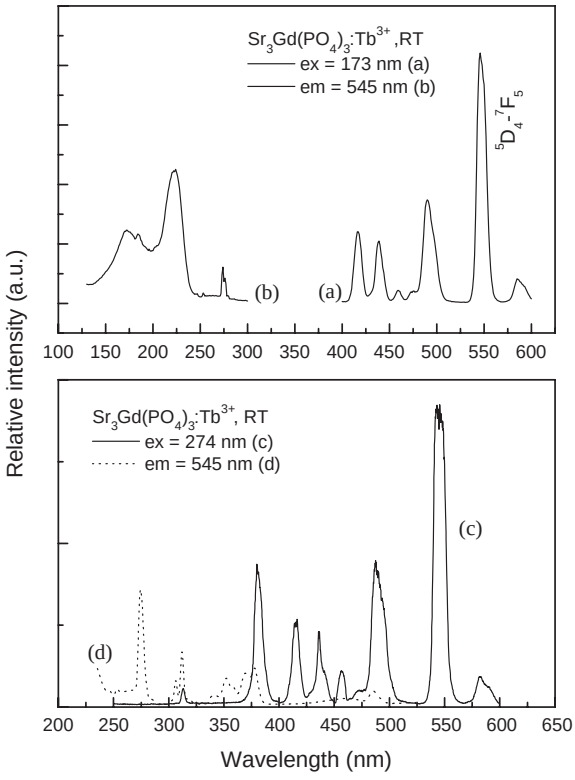


Fig. 6. The VUV excited emission spectrum ((a) excitation under 173 nm), VUV excitation spectrum ((b) under emission at 545 nm), UV excited emission spectrum ((c) excitation under 274 nm) and UV excitation spectrum ((d) under emission at 545 nm) of phosphor $Sr_3Gd_{0.94}Tb_{0.06}(PO_4)_3$ at 293 K.

The ground states ($4f^8$) of $Tb^{3+}$ are $^7F_J$ configurations, when one electron is promoted to $5d$ shell, different with $Ce^{3+}$ and $Pr^{3+}$ ions, it can give rise to two $4f^75d^1$ excitation states: the high-spin states with $^9D_J$ configurations or low-spin states with $^7D_J$ configurations. Obviously, $^9D_J$ states will be lower in energy according to Hund's rule, and the transitions between $^7F_J$ and $^7D_J$ are spin-allowed, while $^7F_J$–$^9D_J$ transitions are spin-forbidden. Therefore, the spin-allowed $f$–$d$ transitions are strong, with higher energy; the spin-forbidden $f$–$d$ transitions are weak, with lower energy. We might firstly estimate the lowest spin-allowed $f$–$d$ transition and the lowest spin-forbidden $f$–$d$ transition of $Tb^{3+}$ using the lowest $5d$ states decrease obtained from $Ce^{3+}$ and $Pr^{3+}$. It is known that when compare with the free ion, the lowest $5d$ states decrease $17.0\times10^3\,cm^{-1}$ for $Ce^{3+}$ and $16.5\times10^3\,cm^{-1}$ for $Pr^{3+}$ in $Sr_3Ln(PO_4)_3$, respectively, and the lowest spin-allowed and spin-forbidden $f$–$d$ transitions for free $Tb^{3+}$ ions was reported to be 62,500 and 56,350 $cm^{-1}$. Hence, the lowest spin-allowed and spin-forbidden $f$–$d$ transition for $Tb^{3+}$ in $Sr_3Ln(PO_4)_3$ is expected to be about $45.5–46.0\times10^3\,cm^{-1}$ (217–220 nm) and $39.4–39.9\times10^3\,cm^{-1}$ (251–254 nm), respectively. Then we might compare these predictions with the spectroscopic figures; the strong bands at 224 in Figs. 5 and 6 and weak band at 260 nm in Fig. 5 is probably assumable to be the lowest spin-allowed and spin-forbidden $f$–$d$ transitions, respectively.

The energies of the lowest $W_{fd(n)}$ of $f^n$-series $RE^{3+}$ ions might be represented as Eq. (1) [30,31].

$$W_{fd(n)} = E(f^{n-1}d) - E(f^n) = V_{fd} + \Delta U(n), \quad (1)$$

where $V_{fd}$ is the single-electron-scheme transition energies from the $4f$-orbit to the $5d$-orbit, and $\Delta U$ the many-electron correction to the single-electron-scheme binding energies. The estimated values of $\Delta U$ for $Ln^{3+}$ ions were reported and listed in Table 3, and the $V_{fd}-n$ correlation was considered to be linear. Therefore, Eqs. (2) and (3) for $RE^{3+}$ in $Sr_3Ln(PO_4)_3$ is obtained by fitted the experimental results. The fitted and predicted lowest $f$–$d$ transitions for $Ln^{3+}$ in host $Sr_3Ln(PO_4)_3$ are listed in Table 3 also, showing the predicted value agrees with the experimental value.

$$V_{fd} = 30.29 + 0.71n \ (\times10^3\,cm^{-1}), \quad (2)$$

$$W_{fd(n)} = 30.29 + 0.71n + \Delta U(n) \ (\times10^3\,cm^{-1}). \quad (3)$$

Table 3
The fitted and predicted lowest $f$–$d$ transitions for $Ln^{3+}$ in hosts $Sr_3Ln(PO_4)_3$

| $n$ | $Ln^{3+}$ | $\Delta U(n)$ ($10^3\,cm^{-1}$) | Predicted ($10^3\,cm^{-1}$) | Experimental ($10^3\,cm^{-1}$) | Relative error (%) |
|---|---|---|---|---|---|
| 1 | $Ce^{3+}$ | 1.2 | 32.20 | 32.258 | 0.18 |
| 2 | $Pr^{3+}$ | 13.4 | 45.11 | 45.045 | −0.14 |
| 8 | $Tb^{3+}$ | 2.5 | 38.47 | 38.461 | −0.02 |

The UV excitation spectrum and emission spectra under VUV-UV excitation are presented in Figs. 5 and 6 also. The UV excitation is in line with the VUV curve in the range of 240–300 nm, weak $f$–$f$ transitions of $Tb^{3+}$ occur in 300–500 nm range of two figures, and the $^8S_{7/2}$–$^6I_{11/2}$ and $^6P_{7/2}$–$^8S_{7/2}$ transitions of $Gd^{3+}$ present in Fig. 6 in $Sr_3Gd(PO_4)_3$:$Tb^{3+}$. Some differences are presented in the emission spectra between the phosphors $Sr_3Tb(PO_4)_3$ and $Sr_3Gd(PO_4)_3$:$Tb^{3+}$ whenever under VUV-UV excitation. The $^5D_3$-$^7F_J$ transitions of $Tb^{3+}$ in 400–450 nm range can be clearly observed in the emission curve of $Sr_3Gd(PO_4)_3$:$Tb^{3+}$, while these transitions are very weak for $Sr_3Tb(PO_4)_3$. This is related to the self-quenching originating from the cross relaxation of $Tb^{3+}$ in pure $Sr_3Tb(PO_4)_3$. The $Tb^{3+}$–$Tb^{3+}$ separation in diluted system $Sr_3Gd(PO_4)_3$:$Tb^{3+}$ is large, and the $^5D_3$–$^7F_J$ blue emission emerged. When the $Tb^{3+}$ concentration increase, the distances between two $Tb^{3+}$ ions decrease, which make $^5D_3$ decay mainly non-radiatively in pure compound $Sr_3Tb(PO_4)_3$ via a cross-relaxation process between transitions $^5D_3$–$^5D_4$ and $^7F_0$–$^7F_6$ of $Tb^{3+}$ [32]. The calculated CIE coordination $x$, $y$ values for $Sr_3Tb(PO_4)_3$ and $Sr_3Gd(PO_4)_3$:$Tb^{3+}$ under VUV-UV excitation are listed in Table 2, the luminescent chromaticity coordinates of NTSC for green are $x = 0.21$, $y = 0.71$, hence the improvement on the color pure for these phosphors is required.

## 4. Conclusions

The VUV-UV excitation spectra and corresponding emission spectra of $Sr_3Gd(PO_4)_3$:$Ln^{3+}$ ($Ln$ = Ce, Pr, Tb) and $Sr_3Ln(PO_4)_3$ ($Ln$ = Ce, Gd, Tb) were determined. The following conclusions could be suggested:

(1) The host lattice absorption band of $Sr_3Ln(PO_4)_3$ peaks near 170 nm as shown from the VUV excitation spectra.
(2) The $f$–$d$ bands for $Ce^{3+}$, $Pr^{3+}$ and $Tb^{3+}$ in $Sr_3Ln(PO_4)_3$ were assigned and corroborated, the lowest $f$–$d$ transition energies ($W_{fd(n)}$) and $n$ value for $4f^n$ configuration $Ln^{3+}$ ions in these host lattices is suggested to be expressed as $W_{fd(n)} = 30.29 + 0.71n + \Delta U(n)$.
(3) The energy transfer occurs among the host lattices, $Gd^{3+}$ and $Ce^{3+}$, $Pr^{3+}$, $Tb^{3+}$ ions. The calculated CIE chromaticity coordinations for the phosphors $Sr_3Gd(PO_4)_3$:$Pr^{3+}$, $Sr_3Gd(PO_4)_3$:$Tb^{3+}$ and $Sr_3Tb(PO_4)_3$ under VUV-UV excitation show small difference with NTSC standard values.

## Acknowledgments

This work is supported by State Key Project of Basic Research of China (G1998061312), National Natural Science Foundation of China (20171046), Guangdong Provincial Natural Science Foundation (001277), Doctorial Training Base Foundation of Ministry of Education of China (20020558034) and the Key Project Foundation of Laboratory of Beijing Synchrotron Radiation (01050), Institute of High Energy Physics, Chinese Academy of Sciences. Rare earth oxides are provided by Yangjiang rare earth factory of Guangdong.

## References

[1] D.J. Segal, R.P. Santoro, R.E. Newnham, Zeit. Kristallog. 123 (1966) 1.
[2] G. Blasse, J. Solid State Chem. 2 (1970) 27.
[3] G. Engel, W. Kirchberger, Z. Anorg. Allg. Chem. 417 (1975) 81.
[4] G.J. McCarthy, J. Solid State Chem. 38 (1981) 128.
[5] P. Fischer, F. Waldner, Solid State Commun. 44 (1982) 657.
[6] T. Tsuboi, H.J. Seo, B.K. Moon, J.H. Kim, Physica B 45 (1999) 270.
[7] E.H. Arbib, B. Elouadi, J.P. Chaminade, J. Darriet, Mater. Res. Bull. 35 (2000) 761.
[8] M.F. Hoogendorp, W.J. Schipper, G. Blasse, J. Alloys Compd. 205 (1994) 249.
[9] T. Znamierowska, W. Szuszkiewicz, J. Hanuza, L. Macalik, D. Hreniak, W. Strek, J. Alloys Compd. 341 (2002) 371.
[10] T. Jüstel, H. Nikol, C. Ronda, Angew. Chem. Int. Ed. 37 (1998) 3084.
[11] K. Sohn, I.W. Zeon, H. Chang, S.K. Lee, H.D. Park, Chem. Mater. 14 (2002) 2140.
[12] J. Zhang, Z. Zhang, Z. Tang, Y. Tao, X. Long, Chem. Mater. 14 (2002) 3005.
[13] A. Meijerink, R.T. Wegh, Mater. Sci. Forum 315–317 (1999) 11.
[14] R.T. Wegh, H. Donker, K.D. Oskam, A. Meijerink, Science 283 (1999) 663.
[15] A.N. Belsky, J.C. Krupa, Displays 19 (1999) 185.
[16] L. Pieterson, M.F. Reid, R.T. Wegh, A. Meijerink, J. Lumin. 94–95 (2001) 79.
[17] L. Pieterson, M.F. Reid, G.W. Burdick, S. Soverna, A. Meijerink, Phys. Rev. B 65 (2002) 045113.
[18] L. Pieterson, M.F. Reid, G.W. Burdick, A. Meijerink, Phys. Rev. B 65 (2002) 045114.
[19] E. Nakazawa, F. Shiga, J. Lumin. 15 (1977) 255.
[20] K.C. Mishra, I. Osterloh, H. Anton, B. Hannebauer, P.C. Schmidt, K.H. Johnson, J. Lumin. 72–74 (1997) 144.
[21] J. Barbier, J.E. Greedan, T. Asaro, G.J. McCarthy, Eur. J. Solid State Inorg. Chem. 27 (1990) 855.
[22] H.B. Liang, Y. Tao, Q. Su, S. Wang, J. Solid State Chem. 167 (2002) 435.

[23] H.B. Liang, Q. Zeng, Y. Tao, S. Wang, Q. Su, Mater. Sci. Eng. B 98 (2003) 213.
[24] H.B. Liang, Y. Tao, Q. Zeng, H. He, S. Wang, X. Hou, W. Wang, Q. Su, Mater. Res. Bull. 38 (2003) 797.
[25] P. Dorenbos, Phys. Rev. B 64 (2001) 125117.
[26] P. Dorenbos, Phys. Rev. B 62 (2000) 15640, 15650.
[27] P. Dorenbos, J. Lumin. 99 (2002) 283.
[28] E. Kolk, P. Dorenbos, A.P. Vink, R.C. Perego, C.W.E. Eijk, Phys. Rev. B 64 (2001) 195129.
[29] A.A. Kaminski, S.E. Sarkisov, G.A. Denisenko, V.V. Ryabchenkov, V.A. Lomonov, Yu.E. Perlin, M.G. Blazha, D. Schultze, B. Hermoneit, P. Reiche, Phys. Stat. Sol. A 85 (1984) 553.
[30] E. Nakazawa, J. Lumin. 100 (2002) 89.
[31] E. Nakazawa, F. Shiga, Jpn. J. Appl. Phys. 42 (2003) 1642.
[32] P. Boutinaud, R. Mahiou, J.C. Cousseins, J. Lumin. 72–74 (1997) 318.